Article

Removal Behavior of Methylene Blue from Aqueous Solution by Tea Waste: Kinetics, Isotherms and Mechanism

Li Liu [1], Shisuo Fan [2],* and Yang Li [3]

[1]   School of Physics and Electronic Engineering, Fuyang Normal University, Fuyang 236037, China;
      wenfan1986@163.com
[2]   School of Resources and Environment, Anhui Agricultural University, Hefei 230036, China
[3]   Guangzhou Key Laboratory of Environmental Catalysis and Pollution Control, School of Environmental
      Science and Engineering, Institute of Environmental Health and Pollution Control, Guangdong University
      of Technology, Guangzhou 510006, China; linziyi_ly@163.com
*   Correspondence: fanshisuo@ahau.edu.cn; Tel./Fax: +86-551-6578-6311

check for
updates

Abstract: Tea waste (biosorbent) was characterized by BET, SEM, FTIR, XPS, solid state ^{13}C-NMR and applied to remove methylene blue (MB) from aqueous solution. The effect of different factors on MB removal, kinetics, isotherms and potential mechanism was investigated. The results showed that tea waste contains multiple organic functional groups. The optimum solid-to-liquid ratio for MB adsorption was $4.0\ g{\cdot}L^{-1}$ and the initial pH of the MB solution did not need to be adjusted to a certain value. The pseudo-second-order model could well fit the adsorption kinetic process. The adsorption process could be divided into two stages: a fast adsorption stage and a slow adsorption stage. The adsorption isotherm could be well described by Langmuir and Temkin isotherm models. The maximum adsorption amount could reach $113.1461\ mg{\cdot}g^{-1}$ based on Langmuir isotherm fitting. Desorption and reusability experiments showed that MB adsorption onto tea waste could be stable and could not cause secondary pollution. The interaction mechanism between tea waste and MB involved electrostatic attraction, hydrogen bond, ion exchange, π-π binding. The organic functional groups of tea waste played an important role during the MB removal process. Therefore, tea waste has the potential to act as an adsorbent to remove MB from aqueous solution.

Keywords: tea waste; methylene blue; kinetics; isotherm; mechanism

1. Introduction

Dyeing industry wastewater can pose a significant risk to the eco-environment due to its color depth, high concentration, complex organic components, toxicity and poor bio-degradability characteristics [1]. Dyeing industry wastewater should be treated before discharge into natural water bodies. However, undesirable or illegal release of wastewater into the environment could also cause serious pollution. Therefore, the treatment of dyeing wastewater is crucial and indispensable.

The main approaches for dyeing industry wastewater disposal include chemical degradation, biological treatment, membrane separation, and adsorption [2]. Compared with other methods, the adsorption technique is currently widely applied to remove pollutants from dyeing wastewater, due to its many advantages, which include easier operation, low cost, and high efficiency [3]. The priority research focuses on the choice of the adsorbent and the investigation of mechanism. Biomass is an ideal material for adsorbent owing to its wide availability and low cost, especially biomass based on agricultural and forestry residues [4–14].

Tea waste is widely produced due to the development of tea industry. Resource utilization of tea waste is a major trend. Preparation of tea waste-based adsorbents had raised intereston account of its characteristics, involving surface structure, functional groups, wide sources, stable removal effect [15]. Tea waste had been prepared as an efficient adsorbent to remove pollutant from aqueous solutions [16]. Removal of dyeing industry wastewater by tea waste had been previously reported and those studies had been focused on adsorption kinetics and thermodynamics [17–19]. However, the adsorption mechanism and recycling utilization of tea waste for methylene blue removal has rarelyreceivedattention. Therefore, the purpose of this study was: (1) to characterize the structure and composition of tea waste; (2) to investigate the adsorption behavior of tea waste for methylene blue adsorption; (3) to explore the adsorption mechanism of tea waste for methylene blue.

2. Materials and Methods

2.1. Materials

Tea waste was collected from a tea factory located at the south of Anhui Province. First, the tea waste was pretreated to remove ash using deionized water. Then, pigments, theophylline and caffeine in the tea waste were eliminated using boiling water. Last, the tea waste was dried at 70 °C and crushed to pass a 100 mesh sieve. The tea waste was then stored for further experiments. The reagents methylene blue (MB), sodium hydroxide, and hydrochloric acid were analytical pure and was purchased from Sinopharm Chemical Reagent Co., Ltd. (Shanghai, China). The experimental water was deoxidized water (membrane treatment).

2.2. Batch Experiment

In each experiment, 20 mL of MB solution was placed in a 50 mL centrifuge tube. The initial concentration of MB solution was diluted to 100 mg·L^{-1} from stock solution (1000 mg·L^{-1}). Different masses of tea waste were added to adjust the solid-to-liquid ratios in the range of 1–10 g·L^{-1} (dosage effect). Meanwhile, the pH value of MB was adjusted to value between 3.0–11.0 with 0.1 M HCl or 0.1 M NaOH solutions to investigate the effect of pH on adsorption. Then, the centrifuge tubes were shaken in a controller shaker (150 rpm) for 24 h at the 35 °C. After centrifugation, the supernatant was passed through a 0.45 µm filter membrane and was collected for measurement. The absorbance of the supernatant was determined by a spectrophotometer at a wavelength of 665 nm. The removal rate and adsorption amount was calculated using the following equations:

$$R = \frac{(C_0 - C_e)}{C_0} \times 100 \tag{1}$$

$$q_e = \frac{(C_0 - C_e) \times V}{m} \tag{2}$$

where R is the removal rate of MB (%). C_0 and C_e are respectively the MB concentrations at the initial time and equilibrium time (mg·L^{-1}). m is the mass of tea waste (mg). V is the solution volume (mL). q_e is the adsorbed amount of MB ontotea waste (mg·g^{-1}).

2.3. Adsorption Kinetics

Based on the above experimental conditions, 100 mL of MB solution with the initial concentration of 100 mg·L^{-1} were placed in a 250 mL conical flask. The pH of the solution was not adjusted. Then, a certain mass of tea waste (0.4 g) was added into the solution and the mixture was agitated at 150 rpm in a shaker at 35 °C. Samples were collected at different timeintervals and analyzed by a spectrophotometer at a wavelength of 665 nm. Then, the amount of MB adsorbed onto he tea waste was calculated. Different kinetic models were applied to fit the adsorption process.

2.4. Adsorption Isotherm

Based on the above experimental conditions, 20 mL of MB solution of different initial concentrations (ranging between 100 and 500 $mg \cdot L^{-1}$) were placed in a 50 mL centrifuge tube. A certain mass of tea waste (0.08 g) was added into the solution in the centrifuge tube and the mixture was agitated at 150 rpm in a shaker at 35 °C for 24 h. The adsorption amount was calculated. Different isotherm models were used to describe the process.

2.5. Characterization

The textural properties of tea waste were analyzed with a surface area and porosity analyzer (Micromeritics TriStar II 3020, Norcross, GA, USA) at 77 K under a N_2 atmosphere. The surface morphology of tea waste was characterized by scanning electron microscopy (HITACHI S-4800, Toyko, Japan).

The concentration of released metals (Ca^{2+}, Na^+, K^+, Mg^{2+}) from the tea waste in the supernatant of the equilibrium solution was analyzed by Inductively Coupled Plasma Optical Emission Spectroscopy (ICP-OES, 2100DV, PerkinElmer, Fremont, CA, USA). The corresponding release of Ca^{2+}, Na^+, K^+, Mg^{2+} from the tea waste with deionzed water was used as control. The functional groups of tea waste were analyzed by Fourier Transform Infrared Spectroscopy (FTIR, Nicolette is50, Thermo Fisher Scientific, Waltham, MA, USA) using the KBr pellet technique. The valence of the C, O, N bound on the tea waste was determined by X-ray Photoelectron Spectrometer (XPS, ESCALAB 250Xi, Thermo Fisher Scientific, Waltham, MA, USA). Nuclear Magnetic Resonance spectra (CP-MAS ^{13}C-NMR) of tea waste were determined at a frequency of 100 MHz using using an Avance III 400 spectrometer (Bruker, Basel, Switzerland). All experiments were run in a double resonance probe head using 4-mm sample rotors. ^{13}C multiple ramped amplitude cross polarization/magic angle spinning (^{13}C multi CP) NMR experiments were performed.

2.6. Desorption and Reusability Experiment

The solutions of MB (initial concentration: 300 $mg \cdot L^{-1}$) were stirred with tea waste (solid-to-liquid ratios: 1 $g \cdot L^{-1}$) for 10 h at 25 °C. The adsorbent was separated from the suspension by mixing with ethanol/acetic acid eluent (*v*/*v*: 9/1) for 10 h and ultrasonicated for 10 min. After ultrasonication the adsorbent was washed with water several times to remove the dye molecules and dried in an oven at 80 °C.

3. Results and Discussion

3.1. Characterization of Tea Waste

The surface area, pore volume and pore diameter of tea waste is 0.913 $m^2 \cdot g^{-1}$, 0.007 $cm^3 \cdot g^{-1}$, 2.611 nm, respectively. Compared with other adsorbents, such as activated carbon, the surface structure of tea waste was not well developed [20]. When tea waste acted as an adsorbent, its adsorption capacity was not limited by its surface structure but also depended on other mechanisms.

A SEM micrograph of tea waste is shown in Figure 1a. Tea waste presented a stem structure due to its main components, including cellulose, and hemicellulose. Tea waste exhibits a heterogeneous or rough and porous (caves) surface structure which was favorable for the the biosorption of MB dye.

The FTIR of tea waste and MB loaded onto tea waste is presented in Figure 1b. The main functional groups of tea waste and MB laden on tea waste are summarized in Table 1. The functional groups of tea waste are as follows: –OH: 3416 cm^{-1}, aliphatic –CH: 2924 cm^{-1} and 2852 cm^{-1}, aromatic C=C and C=O: 1651 cm^{-1}, secondary amine group: 1530 cm^{-1}, N–H bending: 1455 cm^{-1}, –CH$_3$ bending: 1371 cm^{-1}, C–O stretching: 1320 cm^{-1}, –SO$_3$ stretching/P=O: 1237 cm^{-1}, C–O groups: 1150 cm^{-1}, C=O groups: 1036 cm^{-1} [21–24].
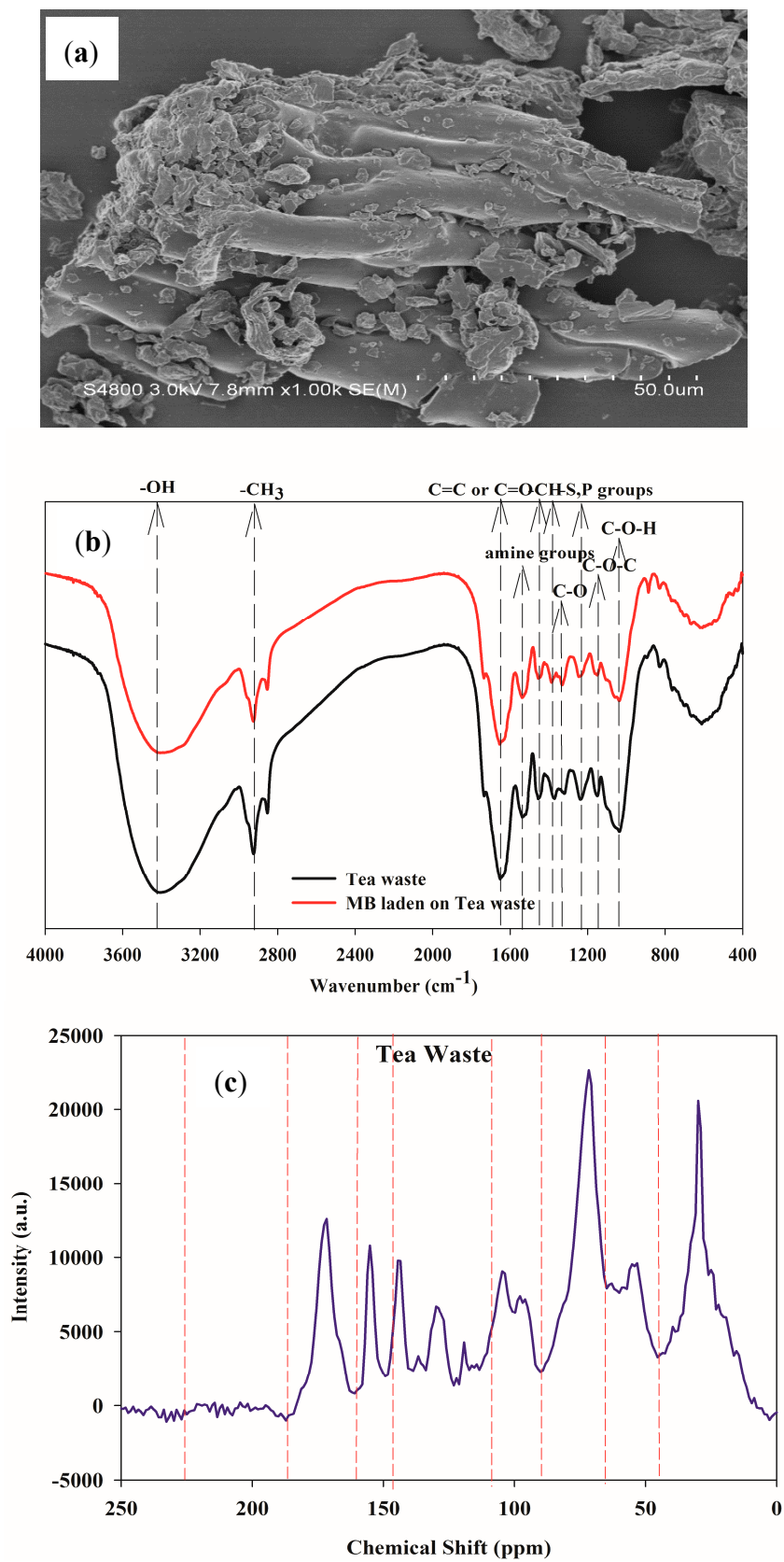
Figure 1. SEM photo (**a**), FTIR (**b**) and ^{13}C-NMR (**c**) of tea waste.

Table 1. Main functional groups of tea waste and MB loaded on tea waste.

Tea Waste			Assignment
Before Adsorption	After Adsorption	Difference	
3416	3406	+17	bonded –OH groups
2924	2925	0	aliphatic C–H group
2852	2852	0	aliphatic C–H group
1651	1644	+7	C=O stretching, Aromatic C=C, C=O/C=C stretching Amid Igroup
1530	1537	−7	secondary amine II group
1455	1455	0	C–H alkanes in aromatic rings
1371	1385	−14	C–H bending,–CH_3 symmetric bending of CH_3
1320	1331	−11	C–O stretching
1237	1244	−4	–SO_3 stretching/P=O or COO vibration
1150	1150	0	C–O–C of polysaccharides
1036	1036	0	C–O–H stretching

When MB was adsorbed onto tea waste, part peaks of functional groups shifted, such as 3416 cm^{-1}→3406 cm^{-1}, 1651 cm^{-1}→1644 cm^{-1}, 1530 cm^{-1}→1537 cm^{-1}, 1371 cm^{-1}→1385 cm^{-1}, 1320 cm^{-1}→1331 cm^{-1}, 1237 cm^{-1}→1244 cm^{-1}. Therefore, the functional groups of –OH, –C=C or C=O, amine groups, –CH in tea waste may participate the interactions with MB, involving the mechanism of surface complex, hydrogen bonding, electrostatic attraction.

Solid state ^{13}C-NMR spectroscopy has emerged as a useful tool to characterize different types of carbon. Figure 1c shows the ^{13}C-NMR spectrumof tea waste. The relative proportion of different carbons in each chemical functional group for the tea waste is presented in Table 2. The relative proportions were integrated in the chemical shift (ppm) resonance intervals of 0–46, 46–65, 65–90, 90–108, 108–145, 145–160, 160–185, 185–225 ppm [25]. Obviously, O-alkyl and alkyl C with the chemical shift of 65–90 ppm and 0–46 ppm were the main C-containing functional groups in tea waste (sum: 46.37%). The O-alkyl and alkyl C refer to carboxyl and hydroxy functional groups. The results were in agreement with the FTIR analysis. Therefore, carbon and oxygen functional groups in tea waste may play a key role during the interaction with MB.

Table 2. Relative proportion of different carbon types in tea waste.

Tea Waste	Chemical Shift (ppm), δ								
	0–46	46–65	65–90	90–108	108–145	145–160	160–185	185–225	225–250
Relative proportion (%)	22.61	12.90	23.76	10.46	14.21	5.71	9.96	0.13	0.26

Note: The spectra were integrated in the chemical shift (ppm) resonance intervals of 0–46 ppm (alkyl C, mainly CH_2 and CH_3 sp[3] carbons), 46–65 ppm (methoxy and N alkyl C from OCH_3, C-N and complex aliphatic carbons), 65–90 ppm (O-alkyl, such as alcohols and ethers), 90–108 ppm (anomeric carbons in carbohydrate-like structure), 108–145 ppm (aromatic and phenolic carbon), 145–160 ppm (oxygen aromatic carbon and olefinic sp[2] carbons), 160–185 ppm (carboxyl, amides and ester) and 185–225 ppm (carboxyls).

The XPS analysis of tea waste is displayed in Figure 2. XPS could provide the information of surface element composition and speciation analysis. As shown in Figure 2a, C, O, N, Fe, Ca, K had been determined by XPS technique. However, Fe, K could not be detected in the tea waste due to the low content. C, O, N, Ca werethe main elements present in the tea waste. According to the XPS peak analysis, high-resolution spectra of C 1s of tea waste could be deconvoluted into three peaks:

284.8, 286.4 and 288.25 eV, which indicates presence of C=C/C–C, C–O–C and O–C=O [26,27]. The O 1s region contained two components, at 532.35 and 533.0 eV, corresponding to C=O and C–O–C or C–OH groups [28,29]. The peaks values are 400.10 and 402.5 eV, corresponding to protonated amine groups and N-H bonds, respectively [30–32]. Ca $2p_{3/2}$ peaks were at 347.4 and 351.20 eV and could be assigned to Ca bound to oxidized carbon, $CaCO_3$ [33]. Therefore, abundant functional groups were present in the tea waste and lead to its adsorption properties.

　　　When the MB was adsorbed onto tea waste, the XPS spectra of tea waste changed as shown in Figure 2b. Compared with raw tea waste, the main speciation of elements in the MB loaded onto tea waste slightly changed. The high-resolution spectra of C 1s of tea waste had been deconvoluted into three peaks: 284.8, 286.35 and 288 eV. The O 1s region contained two components, at 532.40 and 533.0 eV. The peaks values of N are 400.05 and 402.4 eV. Ca 2p3/2 peaks shifted to 347.4 and 351.20 eV. The variation of speciation of element indicated that these organic groups were involved in the interaction between tea waste and MB. The relative content of elements changed. Content of carbon decreased and the content of nitrogen, oxygen increased due to the adsorption of MB.
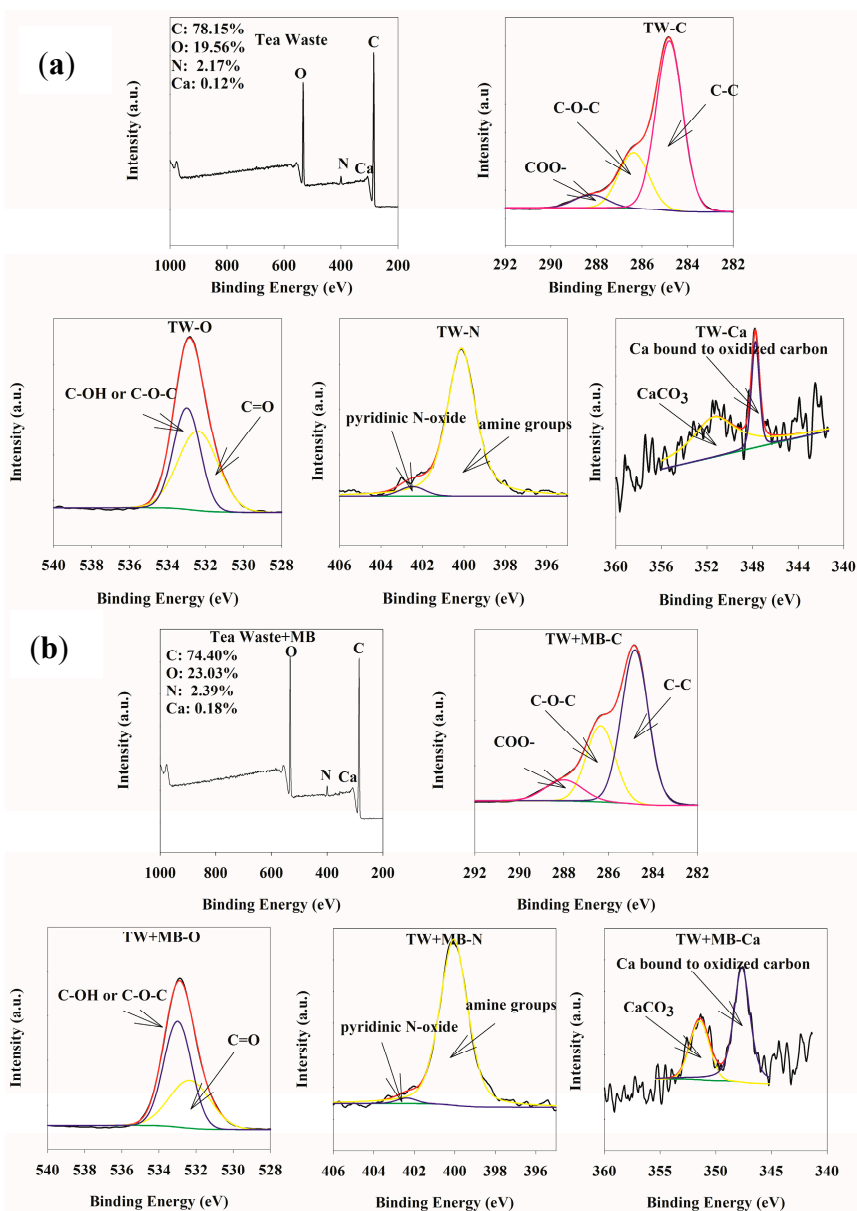

Figure 2. XPS spectra of tea waste (**a**) and MB loaded on tea waste (**b**).

3.2. Adsorption Behavior

3.2.1. Effect of S/L Ratios and pH on MB Adsorption

The effect of solid-to-liquid ratios and pH on MB removal by tea waste is shown in Figure 3. Solid-to-liquid ratio is an important factor influencing the MB removal effect. As shown in Figure 3a, as increase in the S/L ratio initially increased the removal rate of MB. The removal rate plateaued at a solid-to-liquid ratio of 4.0. When the S/L ratio was 4.0, the removal rate reached 98%. Thus, the optimum of S/L was 4.0. Higher S/L ratios indicated more mass of tea waste and could provide more adsorption sites for binding of MB and realized a higher removal effect. When the adsorption reached equilibrium, the removal rate was relative stable.
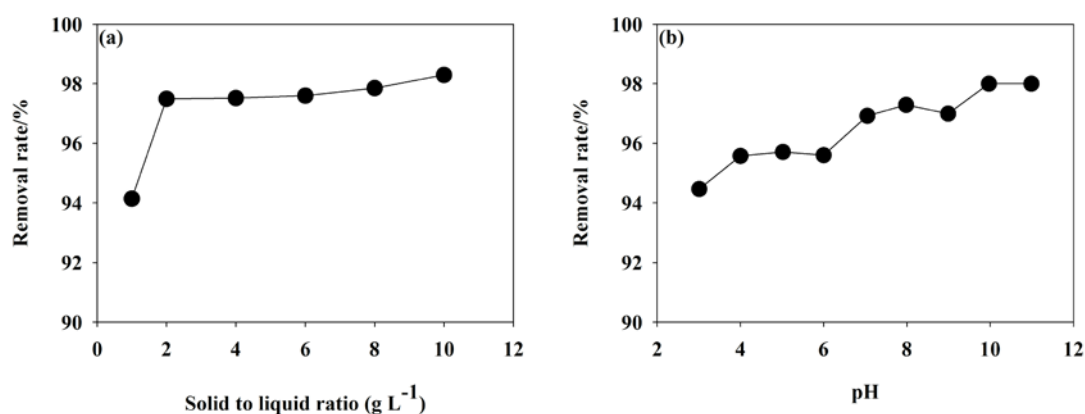

Figure 3. Effect of (**a**) S/L ratio and (**b**) pH on the removal rate of MB.

pH was a key factor during the adsorption process and affected the surface charge of the adsorbent, the degree of ionization, and the speciation of MB in the solution [34]. The effect of pH on MB removal effect is shown in Figure 3b. With increasing of pH the removal rate of pH tended to increase. When the pH was 3.0 and 11.0, the removal rate of MB was 94% and 98%, respectively. The influence of low pH to MB adsorption was that H^+ could occupy the binding sites. This was not favorable for the adsorption of MB [35,36]. Further, MB possessed a positive surface charge and could be repulsed by H^+ to prevent MB adsorption onto tea waste. With increasing pH the number of hydrogen ions in the solution reduced and the competitive effect, repulsive interaction weakened, which may lead to an increase in the removal rate. The MB removal rate became stable when the pH reached 8.0.

In this investigation, the removal rate was larger than 98%, when the pH of solution was not adjusted. Therefore, the pH was not adjusted in the subsequent experiments. Even at low pH value, the removal rate was still high (>94%) and meant other mechanism might be presented during the interaction between tea waste and MB.

3.2.2. Adsorption Kinetics

Adsorption kinetics could be used to investigate the adsorption quantity changes over time and could provide reference for the engineering design process and gain an insight into the adsorption mechanism. In this study, varied nonlinear kinetics models were applied to fit the adsorption process [37–39].

Pseudo first-order model:

$$q_t = q_e(1 - e^{-k_1 t}) \tag{3}$$

where q_e and q_t are the amounts of MB adsorbed (mg·g^{-1}) at equilibrium and at any time t. k_1 is the pseudo first-order rate constant.

Int. J. Environ. Res. Public Health **2018**, *15*, 1321

8 of 16

Pseudo-second-order model:

$$q_t = \frac{k_2 q_e^2 t}{1 + k_2 q_e t} \tag{4}$$

where k_2 is the pseudo-second-order rate constant.

Elovich model [40]:

$$q_t = \frac{1}{\beta} \ln(\alpha\beta) + \frac{1}{\beta} \ln(t) \tag{5}$$

where q_t (mg·g^{-1}) is the same parameters as above mentioned. α (mg/(g·min)$^{-1}$) is the initial adsorption rate, β (g·mg^{-1}) is associate with the fraction of surface coverage and activation energy for chemisorptions.

Two-compartment model (TC model) [41,42]:

$$q_t = q_e(1 - (F_{\text{fast}} e^{-k_{\text{fast}} t} + F_{\text{slow}} e^{-k_{\text{slow}} t})) \tag{6}$$

F_{fast} and F_{slow} are the mass fractions and k_{fast} and k_{slow} are the first-order rate constants for transport into "fast" and "slow" compartment of the adsorbent, respectively.

The nonlinear fitting curve of MB removed by tea waste is displayed in Figure 4a. The fitting parameters of different kinetics models are exhibited in Table 3. Compared with pseudo first-order, Evolich and TC models, the pseudo second-order model could better describe the adsorption process and the correlation coefficient was larger than 0.99. The pseudo-second order modelmeant that adsorption process was controlled by chemisorption which involved valency forces through sharing or exchange of electron between the solvent and the sorbate [43–45]. Because the pseudo-second order model contained the external liquid film diffusion, surface adsorption and intra-particle diffusion processes [46–49], this model could provide a more comprehensive and accurate description of the adsorption mechanism between tea waste and MB.

Table 3. Adsorption kinetics and isotherm parameters of methylene blue on tea waste for various models.

Pseudo-First-Order			Pseudo-Second-Order		
k_1 (L·min^{-1})	q_e (mg·g^{-1})	R^2	k_2 (L·min^{-1})	q_e (mg·g^{-1})	R^2
39.726	23.323	0.9625	0.2317	24.077	0.9908

TC models			Elovich		
		R^2	$\frac{1}{\beta}\ln(\alpha\beta)$	$\frac{1}{\beta}$	R^2
F_{fast}	F_{slow}				
0.7899	0.2101	0.9847	0.0071	11.9523	0.9159
k_{fast}	k_{slow}				
852.8291	20.3117				

Langmuir			Freundlich		
b (L·mg^{-1})	Q_0 (mg·g^{-1})	R^2	K_f	$1/n$	R^2
0.08372	113.1461	0.9748	21.3460	0.3524	0.9159

Temkin			D-R			
b_T (J·mol^{-1})	K_T (L·mg^{-1})	R^2	q_m (mg·g^{-1})	B (mol^2·kJ^{-1})	E (kJ·mol^{-1})	R^2
103.466	0.7790	0.9727	124.1802	1.0330×10^{-8}	6.956	0.9638

Int. J. Environ. Res. Public Health **2018**, *15*, 1321
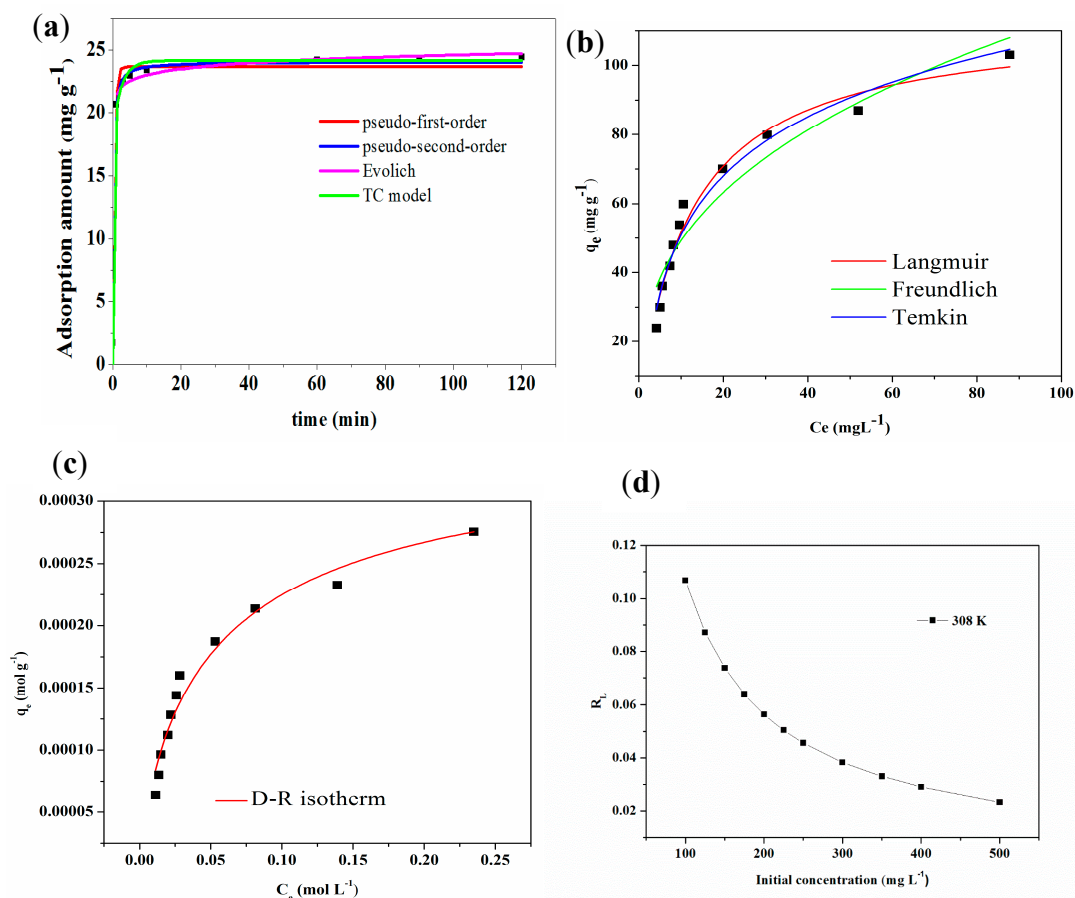
9 of 16

Figure 4. Kinetics (**a**), isotherm (**b**,**c**) curves and (**d**) R_L of MB adsorption by tea waste.

According to the TC models, the adsorption kinetics included an initial fast phase and final slow phase. The fast phase of adsorption could be finished within 5 min and removal rate was more than 90%. The slow phase of adsorption would be accomplished at the remaining time. Based on TC model, the mass fraction of "fast" and "slow" compartment is 78.99% and 21.01%, respectively. The F_{fast} value was greater than 0.5 and larger than those of F_{slow}, indicating that fast adsorption stage was dominant during MB sorption process. Also, the first–order rate constant for transport "fast" compartment (k_{fast}) was obvious lager than those of "slow" compartment (k_{slow}).

3.2.3. Adsorption Isotherm

Adsorption isotherm could be used to study the adsorption mechanism, predict the maximum adsorption capacity of adsorbent, estimate the affinity between adsorbent and adsorbate, optimize the design of adsorption system. In this study, varied nonlinear isotherm models were applied to fit the adsorption process [50], including Langmuir, Freundlich, Dubinin-Radushkevich, Temkin models [51–54]. The nonlinear fitting of the curve of MB remove by tea waste is displayed in Figure 4b,c. The fitting parameters of different isotherm models are listed in Table 3.

Langmuir model:

$$q_e = \frac{Q_0 b_L C_e}{1 + b_L C_e} \tag{7}$$

where C_e is the equilibrium concentration of MB (mg·L^{-1}), q_e is the amount of MB adsorbed per gram adsorbent at equilibrium (mg·g^{-1}). Q_0 is maximum adsorption capacity (mg·g^{-1}), b_L is the Langmuir isotherm constant (L·mg^{-1}).

Langmuir could be fitted well to the adsorption process and the maximum adsorption capacity was 113.1461 mg·g^{-1}. The potential of tea waste can be evaluated by comparing the adsorption capacity of MB onto various adsorbents (based on tea waste biomass) as shown in Table 4. The performance of the tea waste is clearly seen to be considerably effective for MB removal.

Table 4. Comparison of MB sorption capacity of tea waste with that of different sorbents-based on tea waste (Q_0 obtained from Langmuir fitting).

Adsorbent	Q_0 (mg·g^{-1})	pH	References
rejected tea (particle size in the range 250–355 μm)	147 (30 °C), 154 (40 °C), 156 (50 °C)	pH of 6–7	[11]
spent tea leaves (0.5–1.0 mm)	300.052	without changing the solution pH	[12]
tea waste (180–300 μm)	85.16	pH of 8	[13]
NaOH-modified rejected tea	242.11	pH of 7	[14]
Tea waste (less than 150 μm)	113.1461	pH unadjusted	This study

Dimensionless equilibrium constant, R_L, referred to as the separate factor:

$$R_L = \frac{1}{1 + b_L C_i} \tag{8}$$

where C_i is the initial concentration of MB (mg·L^{-1}).

The value of R_L lies between 0 and 1 for favorable adsorption, while $R_L > 1$ means unfavorable adsorption, and $R_L = 1$ represents linear adsorption while the adsorption process is irreversible if $R_L = 0$ [55]. As shown in Figure 4d, R_L is less than 1 in this investigation and demonstrates that adsorption process is effective and beneficial. Increased MB concentration could be beneficial for the adsorption behavior.

Freundlich model:

$$q_e = K_F C_e^{1/n} \tag{9}$$

where q_e is the amount of MB adsorbed per unit weight of adsorbent (mg·g^{-1}), C_e is the equilibrium concentration of solute in the bulk solution (mg·L^{-1}). K_F is the constant indicative of the relative adsorption capacity of the adsorbent (mg·g^{-1}) and $1/n$ is the constant representing the intensity of the adsorption.

$1/n$ in Freundlich equation could reflect the difficulty of adsorption behavior. Generally, when $1/n$ is less than 0.5, the adsorption process would be easily carried out. Adsorption process is difficult when the $1/n$ is larger than 0.5 [4,5]. In this research, the $1/n$ is less than 0.5 when MB was adsorbed onto tea waste, suggesting that adsorption behavior of methylene blue on tea waste easily performed.

Dubinin-Radushkevich model:

$$q_e = Q_m e^{K\varepsilon^2} \tag{10}$$

$$\varepsilon = RT \ln(1 + \frac{1}{C_e}) \tag{11}$$

$$E = \frac{1}{\sqrt{2K}} \tag{12}$$

where K donates the coefficient related to the mean free energy of adsorption (mol^2·kJ^2), Q_m is the maximum adsorption capacity (mg·g^{-1}), and ε is the Polanyi potential, calculated by the equation. R

is the gas constant (8.314 J·(mol·K)$^{-1}$) and T is the absolute temperature (K). The mean adsorption energy E is calculated by the use of K values.

The mean adsorption energy provides important information related to the physical and chemical nature of the adsorption process. E is in the range of 8 kJ·mol^{-1}, 8–16 kJ·mol^{-1}, 16–40 kJ·mol^{-1}, it corresponds to the physical interaction, ion exchange, chemical interaction, respectively [23]. In this study, the E of MB adsorbed on tea waste is 6.956 kJ·mol^{-1}, indicating that physical interactions could play an important role during the adsorption process.

Temkin model:

$$q_e = \frac{RT}{b_T} \ln(A_T C_e) \tag{13}$$

where A_T, Temkin isotherm equilibrium binding constant (L·mg^{-1}) and b_T, Temkin isotherm constant (J·mol^{-1}).

The Temkin isotherm model assumes that the heat of adsorption of all the molecules in the layer decreases linearly with coverage due to adsorbent–adsorbate interactions and mainly describes the chemisoprtion process which dominated through electrostatic adsorption [4,5]. In this investigation, the correlation coefficient of Temkin model was larger than 0.95, revealing that electrostatic interaction was an important mechanism between tea waste and methylene blue.

3.3. Desorption and Reusability Performance

Desorption and reusability properties are important indicators to assess the stability of adsorbent. The reusability of tea waste towards adsorption of methylene blue dye molecules was studied for three cycles. The adsorption of MB (initial concentration: 300 mg·L^{-1}) was stirred with the tea waste (solid-to-liquid ratios: 1 g·L^{-1}) for 10 h at 25 °C. The adsorbent was separated from the suspension by mixing with ethanol/acetic acid eluent (*v/v*: 9/1) for 10 h and ultrasonicated for 10 min. After ultrasonication, the adsorbent was washed with water for several times to remove the dye molecules and dried in an oven at 80 °C.

The removal rate of MB by tea waste is shown in Figure 5. The removal rate dropped to about 30% after three cycles. The removal rate of desorbed-tea waste decreased due to the change of superficial structure of tea waste and loss of the binding site in tea waste. In previous research, decrease of removal rate could be attributed the solubilized some parts of tea waste, changed superficial structures of tea waste and subsequently led to loss or blockage of adsorption sites [56,57]. Meanwhile, the desorption experiment indicated that tea waste had the potential to be adsorbent for MB removal and could not cause secondary pollution.
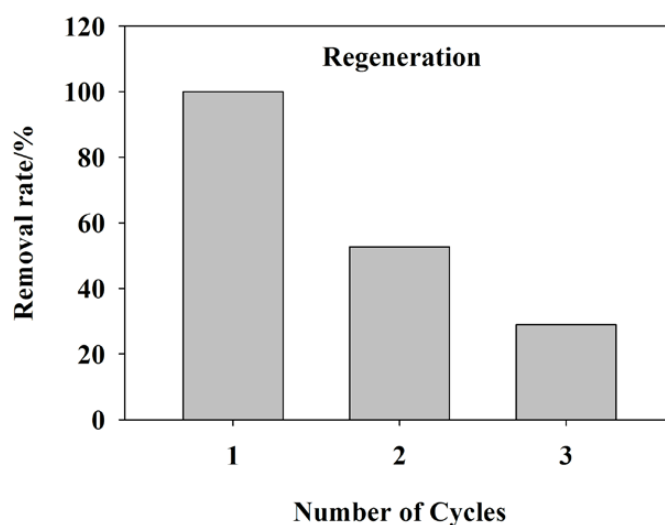

Figure 5. Desorption and reusability study for adsorption of methyl blue onto tea waste.

3.4. Recommended Adsorption Mechanism

The results of different factors on MB adsorption, adsorption kinetics and isotherm are summarized. The above analysis shows that the adsorption of methylene blue onto tea waste was a complicated process, involving multiple steps and various interactions.

Based on the results of TC models, the adsorption process could be divided into fast stage and slow stage. The fast adsorption stage could be finished in 5 min and the removal rate reached 79%. The slow adsorption stage could be accomplished by the remaining time and the removal rate is 21%. The fast adsorption stage could be explained by the following reason: the electrostatic ion exchange between MB and organic functional groups derived from tea waste is commonly considered to be fast and may reach higher removal rate in few minutes. Meanwhile, hydrogen bond or π-π stacking interaction between MB and tea waste may also exist during the adsorption process. This result was consistent with the analysis of the material by FTIR and XPS, which showed that organic functional groups obvious shifted after MB adsorbed onto tea waste. Therefore, organic functional groups of tea waste played an important role during the MB adsorption.

The pseudo second-order model could fit the kinetics data of MB adsorption onto tea waste, suggesting that chemisorptioninteractions play a dominant role during the adsorption process. Meanwhile, the interaction between tea waste and MB involved physical mechanism on account of E derived from D-R model. According to the results of pH effect, electrostatic interaction existed between tea waste and methylene blue. However, the electrostatic interaction was not the sole mechanism.

The MB molecular could occur with tea waste through surface complextion and H^+, Ca^{2+}, Mg^{2+} ions could be released into the solution. The decrease of pH from and cation detected in the solution could confirm the mechanism. When the adsorption process reached equilibrium, the pH of methylene blue solution from 7.98, 7.05, 6.00 decreased to 6.64, 5.98, 5.20 based on the results of pH measurement. Cation exchange was an important mechanism for adsorption of MB onto the tea waste surface. According to previous research, cation exchange is a key mechanism for MB adsorption onto adsorbent [58]. The net amount of released cations (mequiv·g^{-1}) was calculated and is presented in Table 5. As seen in Table 5, net amount of released cations increased after MB adsorption and indicated that more cations were released to supernatant, especially the Ca^{2+} and Na^+ ions which more participates the ion exchange process.

Table 5. The release of Ca^{2+}, Mg^{2+}, Na^+, K^+ during MB adsorption by tea waste at 35 °C.

Samples	The Net Amountof Released Cations (Mequivg^{-1})				Sum
	Ca^{2+}	K^+	Mg^+	Na^+	
100 mg·L^{-1}–35 °C	0.02545	−0.00679	0.001938	0.073848	0.09444
100 mg·L^{-1}–45 °C	0.0157188	−0.00955	0.002167	0.05962	0.067954
100 mg·L^{-1}–45 °C	0.0186688	−0.01212	0.002333	0.055554	0.064441

Note: 100 mg·L^{-1}–35 °C means the concentration of MB was 100 mg·L^{-1} and the operating temperature was 35 °C during the adsorption kinetics experiment.

The two benzene rings contained in methylene blue easily form π-π stacking interaction with the aromatic rings in the tea waste [59]. In short, the interaction between tea waste and MB referred to various mechanisms, including electrostatic interaction, hydrogen bond, ion exchange, π-π binding. Other research also found the similar mechanism [59–64]. The recommended mechanism diagram is displayed in Figure 6.

Figure 6. Mechanism diagram between tea waste and methylene blue.

3.5. Environmental Significance of This Work

Large amounts of tea waste were produced in our province. Tea waste could be collected from tea factories or surrounding residents. Tea waste was washed with water to remove impurities. Then, tea waste could be dried through solar energy drying. The dried tea waste was crushed using a grinder. Pulverized tea waste could be sent to dyeing industries in local area and could be acted as an adsorbent to remove dyeing industry wastewater. Tea waste collection system and crushing treatment are the primary cost analysis. This cost could be compensated through dyeing industry wastewater treatment and tea waste disposal. Hence, large scale application of tea waste as low cost adsorbent is possible.

4. Conclusions

The kinetics process of MB adsorbed onto tea waste could be well described by a pseudo-second-order model. The kinetics process could be divided into a fast stage and a slow stage. The fast stage of adsorption could be finished within 5 min and removal rate was more than 90%. Langmuir could better fit the isotherm model and the maximum adsorption capacity is 113.1461 mg·g^{-1}. The interaction between tea waste and MB referred to various mechanisms, including electrostatic interaction, hydrogen bond, ion exchange, π-π binding. Organic functional groups of tea waste played an important role during the MB adsorption. Therefore, tea waste could be acted as a potential adsorbent to remove dyeing wastewater.

References

1.　Forgacs, E.; Cserháti, T.; Oros, G. Removal of synthetic dyes from wastewaters: A review. *Environ. Int.* **2004**, *30*, 953–971. [CrossRef] [PubMed]

Int. J. Environ. Res. Public Health **2018**, *15*, 1321

14 of 16

2.   Robinson, T.; Mcmullan, G.; Marchant, R.; Nigam, P. Remediation of dyes in textile effluent: A critical review on current treatment technologies with a proposed alternative. *Bioresour. Technol.* **2001**, *77*, 247–255. [CrossRef]

3.   Crini, G. Non-conventional low-cost adsorbents for dye removal: A review. *Bioresour. Technol.* **2006**, *97*, 1061–1085. [CrossRef] [PubMed]

4.   Li, S.; Qian, K.; Wang, S.; Liang, K.; Yan, W. Polypyrrole-Grafted Coconut Shell Biological Carbon as a Potential Adsorbent for Methyl Tert-Butyl Ether Removal: Characterization and Adsorption Capability. *Int. J. Environ. Res. Public Health* **2017**, *14*, 113. [CrossRef] [PubMed]

5.   Mayacela Rojas, C.M.; Rivera Velásquez, M.F.; Tavolaro, A.; Molinari, A.; Fallico, C. Use of Vegetable Fibers for PRB to Remove Heavy Metals from Contaminated Aquifers-Comparisons among Cabuya Fibers, Broom Fibers and ZVI. *Int. J. Environ. Res. Public Health* **2017**, *14*, 684. [CrossRef] [PubMed]

6.   Mu'Azu, N.D.; Jarrah, N.; Zubair, M.; Alagha, O. Removal of Phenolic Compounds from Water Using Sewage Sludge-Based Activated Carbon Adsorption: A Review. *Int. J. Environ. Res. Public Health* **2017**, *14*, 1094. [CrossRef] [PubMed]

7.   Lee, M.E.; Park, J.H.; Chung, J.W. Adsorption of Pb(II) and Cu(II) by Ginkgo-Leaf-Derived Biochar Produced under Various Carbonization Temperatures and Times. *Int. J. Environ. Res. Public Health* **2017**, *14*, 1528. [CrossRef] [PubMed]

8.   Song, R.; Yang, S.; Xu, H.; Wang, Z.; Chen, Y.; Wang, Y. Adsorption Behavior and Mechanism for the Uptake of Fluoride Ions by Reed Residues. *Int. J. Environ. Res. Public Health* **2018**, *15*, 101. [CrossRef] [PubMed]

9.   Wang, D.; Xu, H.; Yang, S.; Wang, W.; Wang, Y. Adsorption Property and Mechanism of Oxytetracycline onto Willow Residues. *Int. J. Environ. Res. Public Health* **2017**, *15*, 8. [CrossRef] [PubMed]

10. Chew, S.Y.; Ting, A.S.Y. Common filamentous *Trichoderma asperellum* for effective removal of triphenylmethane dyes. *Desalin. Water Treat.* **2016**, *57*, 13534–13539. [CrossRef]

11. Alqadami, A.A.; Naushad, M.; Abdalla, M.A.; Khan, M.R.; Alothman, Z.A. Adsorptive Removal of Toxic Dye Using Fe_3O_4–TSC Nanocomposite: Equilibrium, Kinetic, and Thermodynamic Studies. *J. Chem. Eng. Data* **2016**, *61*, 3806–3813. [CrossRef]

12. Zaini, M.A.A.; Salleh, L.M.; Azizi, M.; Yunus, C.; Naushad, M. Potassium hydroxide-treated palm kernel shell sorbents for the efficient removal of methyl violet dye. *Desalin. Water Treat.* **2017**, *84*, 262–270.

13. Albadarin, A.B.; Charara, M.; Abu Tarboush, B.J.; Ahmad, M.N.M.; Kurniawan, T.A.; Naushad, M.; Walker, G.M.; Mangwandi, C. Mechanism analysis of tartrazine biosorption onto masau stones; a low cost by-product from semi-arid regions. *J. Mol. Liq.* **2017**, *242*, 478–483. [CrossRef]

14. Xu, H.; Guo, L. Molecular size-dependent abundance and composition of dissolved organic matter in river, lake and sea waters. *Water Res.* **2017**, *117*, 115–126. [CrossRef] [PubMed]

15. Sud, D.; Mahajan, G.; Kaur, M.P. Agricultural waste material as potential adsorbent for sequestering heavy metal ions from aqueous solutions—A review. *Bioresour. Technol.* **2008**, *99*, 6017–6027. [CrossRef] [PubMed]

16. Nasuha, N.; Hameed, B.H.; Din, A.T. Rejected tea as a potential low-cost adsorbent for the removal of methylene blue. *J. Hazard. Mater.* **2010**, *175*, 126–132. [CrossRef] [PubMed]

17. Hameed, B.H. Spent tea leaves: A new non-conventional and low-cost adsorbent for removal of basic dye from aqueous solutions. *J. Hazard. Mater.* **2009**, *161*, 753–759. [CrossRef] [PubMed]

18. Uddin, M.T.; Islam, M.A.; Mahmud, S.; Rukanuzzaman, M. Adsorptive removal of methylene blue by tea waste. *J. Hazard. Mater.* **2009**, *164*, 53–60. [CrossRef] [PubMed]

19. Nasuha, N.; Hameed, B.H. Adsorption of methylene blue from aqueous solution onto NaOH-modified rejected tea. *Chem. Eng. J.* **2011**, *166*, 783–786. [CrossRef]

20. An, I.A.W.; Ahmad, A.L.; Hameed, B.H. Adsorption of basic dye on high-surface-area activated carbon prepared from coconut husk: Equilibrium, kinetic and thermodynamic studies. *J. Hazard. Mater.* **2008**, *154*, 337–346.

21. Eroğlu, H.; Yapici, S.; Nuhoğlu, Ç.; Varoğlu, E. An environmentally friendly process; adsorption of radionuclide Tl-201 on fibrous waste tea. *J. Hazard. Mater.* **2008**, *163*, 607–617. [CrossRef] [PubMed]

22. Özbaş, E.E.; Öngen, A.; Gökçe, C.E. Removal of astrazon red 6B from aqueous solution using waste tea and spent tea bag. *Desalin. Water Treat.* **2013**, *51*, 7523–7535. [CrossRef]

23. Fan, S.; Tang, J.; Wang, Y.; Li, H.; Zhang, H.; Tang, J.; Wang, Z.; Li, X. Biochar prepared from co-pyrolysis of municipal sewage sludge and tea waste for the adsorption of methylene blue from aqueous solutions: Kinetics, isotherm, thermodynamic and mechanism. *J. Mol. Liq.* **2016**, *220*, 432–441. [CrossRef]

24. Fan, S.; Wang, Y.; Li, Y.; Tang, J.; Wang, Z.; Tang, J.; Li, X.; Hu, K. Facile synthesis of tea waste/Fe_3O_4 nanoparticle composite for hexavalent chromium removal from aqueous solution. *RSC Adv.* **2017**, *7*, 7576–7590. [CrossRef]

25. Zhao, L.; Cao, X.D.; Mašek, O.; Zimmerman, A. Heterogeneity of biochar properties as a function of feedstock sources and production temperatures. *J. Hazard. Mater.* **2013**, *256–257*, 1–9. [CrossRef] [PubMed]

26. Tang, C.; Shu, Y.; Zhang, R.; Li, X.; Song, J.; Li, B.; Zhang, Y.; Ou, D. Comparison of the removal and adsorption mechanisms of cadmium and lead from aqueous solution by activated carbons prepared from *Typha angustifolia* and *Salix matsudana*. *RSC Adv.* **2017**, *7*, 16092–16103. [CrossRef]

27. Chen, S.-Q.; Chen, Y.-L.; Jiang, H. Slow Pyrolysis Magnetization of Hydrochar for Effective and Highly Stable Removal of Tetracycline from Aqueous Solution. *Ind. Eng. Chem. Res.* **2017**, *56*, 3059–3066. [CrossRef]

28. Rodrigues, R.; Gonçalves, M.; Mandelli, D.; Pescarmona, P.P.; Carvalho, W.A. Solvent-free conversion of glycerol to solketalcatalysed by activated carbons functionalised with acid groups. *Catal. Sci. Technol.* **2014**, *4*, 2293–2301. [CrossRef]

29. Milczarek, G.; Ciszewski, A.; Stepniak, I. Oxygen-doped activated carbon fiber cloth as electrode material for electrochemical capacitor. *J. Power Sources* **2011**, *196*, 7882–7885. [CrossRef]

30. Zhao, L.; Baccile, N.; Gross, S.; Zhang, Y.; Wei, W.; Sun, Y.; Antonietti, M.; Titirici, M.M. Sustainable nitrogen-doped carbonaceous materials from biomass derivatives. *Carbon* **2010**, *48*, 3778–3787. [CrossRef]

31. Wohlgemuth, S.A.; Vilela, F.; Titirici, M.M.; Antonietti, M. A one-pot hydrothermal synthesis of tunable dual heteroatom-doped carbon microspheres. *Green Chem.* **2012**, *14*, 741–749. [CrossRef]

32. Mo, Z.; Liao, S.; Zheng, Y.; Fu, Z. Preparation of nitrogen-doped carbon nanotube arrays and their catalysis towards cathodic oxygen reduction in acidic and alkaline media. *Carbon* **2012**, *50*, 2620–2627. [CrossRef]

33. Archanjo, B.S.; Araujo, J.R.; Silva, A.M.; Capaz, R.B.; Falcão, N.P.S.; Jorio, A.; Achete, C.A. Chemical Analysis and Molecular Models for Calcium–Oxygen–Carbon Interactions in Black Carbon Found in Fertile Amazonian Anthrosoils. *Environ. Sci. Technol.* **2014**, *48*, 7445–7452. [CrossRef] [PubMed]

34. Kołodyńska, D.; Wnętrzak, R.; Leahy, J.J.; Hayes, M.H.B.; Kwapiński, W.; Hubicki, Z. Kinetic and adsorptive characterization of biochar in metal ions removal. *Chem. Eng. J.* **2012**, *197*, 295–305. [CrossRef]

35. Zhao, L.; Yang, S.T.; Feng, S.; Ma, Q.; Peng, X.; Wu, D. Preparation and Application of Carboxylated Graphene Oxide Sponge in Dye Removal. *Int. J. Environ. Res. Public Health* **2017**, *14*, 1301. [CrossRef] [PubMed]

36. Ma, L.; Jiang, C.; Lin, Z.; Zou, Z. Microwave-Hydrothermal Treated Grape Peel as an Efficient Biosorbent for Methylene Blue Removal. *Int. J. Environ. Res. Public Health* **2018**, *15*, 239. [CrossRef] [PubMed]

37. Lagergren, S. About the theory of so-called adsorption of soluble substances. *Kungliga Svenska Ventenskapsakademiens Handlingar* **1898**, *24*, 1–39.

38. Ho, Y.S.; Mckay, G. A kinetic study of dye sorption by biosorbent waste product pith. *Resour. Conserv. Recycl.* **1999**, *25*, 171–193. [CrossRef]

39. Ho, Y.S.; Mckay, G. Pseudo-second order model for sorption processes. *Process Biochem.* **1999**, *34*, 451–465. [CrossRef]

40. Chien, S.H.; Clayton, W.R. Application of Elovich equation to the kinetics of phosphate release and sorption in soils. *Soil Sci. Soc. Am. J.* **1980**, *44*, 265–268. [CrossRef]

41. Wang, Z.; Liu, G.; Zheng, H.; Li, F.; Ngo, H.H.; Guo, W.; Liu, C.; Chen, L.; Xing, B. Investigating the mechanisms of biochar's removal of lead from solution. *Bioresour. Technol.* **2015**, *177*, 308–317. [CrossRef] [PubMed]

42. Chen, Z.; Chen, B.; Chiou, C.T. Fast and Slow Rates of Naphthalene Sorption to Biochars Produced at Different Temperatures. *Environ. Sci. Technol.* **2012**, *46*, 11104–11111. [CrossRef] [PubMed]

43. Sun, Y.; Ding, C.; Cheng, W.; Wang, X. Simultaneous adsorption and reduction of U(VI) on reduced graphene oxide-supported nanoscale zerovalent iron. *J. Hazard. Mater.* **2014**, *280*, 399–408. [CrossRef] [PubMed]

44. Al-Ghouti, M.A.; Khraisheh, M.A.; Ahmad, M.N.; Allen, S. Adsorption behaviour of methylene blue onto Jordanian diatomite: A kinetic study. *J. Hazard. Mater.* **2008**, *165*, 589–598. [CrossRef] [PubMed]

45. Malash, G.F.; Elkhaiary, M.I. Methylene blue adsorption by the waste of Abu-Tartour phosphate rock. *J. Colloid Interface Sci.* **2010**, *348*, 537–545. [CrossRef] [PubMed]

46. Sun, L.; Wan, S.; Luo, W. Biochars prepared from anaerobic digestion residue, palm bark, and eucalyptus for adsorption of cationic methylene blue dye: Characterization, equilibrium, and kinetic studies. *Bioresour. Technol.* **2013**, *140*, 406–413. [CrossRef] [PubMed]

Int. J. Environ. Res. Public Health **2018**, *15*, 1321

16 of 16

47. Wang, X.; Liu, N.; Liu, Y.; Jiang, L.; Zeng, G.; Tan, X.; Liu, S.; Yin, Z.; Tian, S.; Li, J. Adsorption Removal of 17β-Estradiol from Water by Rice Straw-Derived Biochar with Special Attention to Pyrolysis Temperature and Background Chemistry. *Int. J. Environ. Res. Public Health* **2017**, *14*, 1213. [CrossRef] [PubMed]

48. Zhang, X.; Wang, X.; Chen, Z. Radioactive Cobalt(II) Removal from Aqueous Solutions Using a Reusable Nanocomposite: Kinetic, Isotherms, and Mechanistic Study. *Int. J. Environ. Res. Public Health* **2017**, *14*, 1453. [CrossRef] [PubMed]

49. Hu, X.; Zhao, Y.; Wang, H.; Tan, X.; Yang, Y.; Liu, Y. Efficient Removal of Tetracycline from Aqueous Media with a Fe_3O_4Nanoparticles@graphene Oxide Nanosheets Assembly. *Int. J. Environ. Res. Public Health* **2017**, *14*, 1495. [CrossRef] [PubMed]

50. Foo, K.Y.; Hameed, B.H. Insights into the modeling of adsorption isotherm systems. *Chem. Eng. J.* **2010**, *156*, 2–10. [CrossRef]

51. Langmuir, I. The constitution and fundamental properties of solids and liquids. Part II.—Liquids. *J. Am. Chem. Soc.* **1916**, *38*, 102–105. [CrossRef]

52. Freundlich, H. Über die Adsorption in Lösungen: ZeitschriftfürphysikalischeChemie. *J. Am. Chem. Soc.* **1906**, *62*, 121–125. [CrossRef]

53. Dubinin, M.M.; Radushkevich, L.V. Equation of the Characteristic Curve of Activated Charcoal. *Proc. Acad. Sci. Phys. Chem. Sect.* **1947**, *55*, 331–337.

54. Temkin, M.; Pyzhev, V. Recent modifications to Langmuir isotherms. *Acta Physicochim. USSR* **1940**, *12*, 217–225.

55. Hall, K.R.; Eagleton, L.C.; Acrivos, A.; Vermeulen, T. Pore- and Solid-Diffusion Kinetics in Fixed-Bed Adsorption under Constant-Pattern Conditions. *Ind. Eng. Chem. Fundam.* **1966**, *5*, 587–594. [CrossRef]

56. Wang, S.Y.; Tang, Y.K.; Chen, C.; Wu, J.T.; Huang, Z.; Mo, Y.Y.; Zhang, K.X.; Chen, J.B. Regeneration of magnetic biochar derived from eucalyptus leaf residue for lead(II) removal. *Bioresour. Technol.* **2015**, *186*, 360–364. [CrossRef] [PubMed]

57. Daneshvar, E.; Vazirzadeh, A.; Niazi, A.; Kousha, M.; Naushad, M.; Bhatnagar, A. Desorption of Methylene blue dye from brown macroalga: Effects of operating parameters, isotherm study and kinetic modeling. *J. Clean. Prod.* **2017**, *152*, 443–453. [CrossRef]

58. Zhu, S.; Fang, S.; Huo, M.; Yu, Y.; Chen, Y.; Yang, X.; Geng, Z.; Wang, Y.; Bian, D.; Huo, H. A novel conversion of the groundwater treatment sludge to magnetic particles for the adsorption of methylene blue. *J. Hazard. Mater.* **2015**, *292*, 173–179. [CrossRef] [PubMed]

59. Vargas, A.M.M.; Cazetta, A.L.; Kunita, M.H.; Silva, T.L.; Almeida, V.C. Adsorption of methylene blue on activated carbon produced from flamboyant pods (*Delonix regia*): Study of adsorption isotherms and kinetic models. *Chem. Eng. J.* **2011**, *168*, 722–730. [CrossRef]

60. Shao, Y.; Zhou, L.; Bao, C.; Ma, J.; Liu, M.; Wang, F. Magnetic responsive metal–organic frameworks nanosphere with core–shell structure for highly efficient removal of methylene blue. *Chem. Eng. J.* **2016**, *283*, 1127–1136. [CrossRef]

61. Altenor, S.; Carene, B.; Emmanuel, E.; Lambert, J.; Ehrhardt, J.J.; Gaspard, S. Adsorption studies of methylene blue and phenol onto vetiver roots activated carbon prepared by chemical activation. *J. Hazard. Mater.* **2008**, *165*, 1029–1039. [CrossRef] [PubMed]

62. Li, G.; Zhu, W.; Zhang, C.; Zhang, S.; Liu, L.; Zhu, L.; Zhao, W. Effect of a magnetic field on the adsorptive removal of methylene blue onto wheat straw biochar. *Bioresour. Technol.* **2016**, *206*, 16–22. [CrossRef] [PubMed]

63. Ai, L.; Zhang, C.; Liao, F.; Wang, Y.; Li, M.; Meng, L.; Jiang, J. Removal of methylene blue from aqueous solution with magnetite loaded multi-wall carbon nanotube: Kinetic, isotherm and mechanism analysis. *J. Hazard. Mater.* **2012**, *198*, 282–290. [CrossRef] [PubMed]

64. Albadarin, A.B.; Collins, M.N.; Naushad, M.; Shirazian, S.; Walker, G.; Mangwandi, C. Activated lignin-chitosan extruded blends for efficient adsorption of methylene blue. *Chem. Eng. J.* **2017**, *307*, 264–272. [CrossRef]